Wave dispersion in gyrotropic relativistic pulsar plasmas

Q. Luo,* D. B. Melrose, and D. Fussell
Research Centre for Theoretical Astrophysics, School of Physics, University of Sydney, New South Wales 2006, Australia
(Received 20 March 2002; published 15 August 2002)

Wave dispersion in a gyrotropic relativistic pulsar plasma is discussed. A pulsar plasma in general contains electrons, positrons, and possibly ions. Although electron-positron pairs are dominant in number density, charge neutrality is generally not satisfied and the gyrotropic terms need to be considered. These gyrotropic terms can lead to elliptical polarization that may be relevant for the observed circular polarization of pulsar radio emission. The wave dispersion and polarization are obtained numerically by calculating the response in terms of the three relativistic plasma dispersion functions. For waves propagating at an oblique angle (to the ambient magnetic field) a significant ellipticity requires the plasma to deviate substantially from the neutrality condition.

DOI: 10.1103/PhysRevE.66.026405 PACS number(s): 52.27.Ny, 52.27.Ep, 52.35.Ra, 52.35.Mw

I. INTRODUCTION

The mechanism of pulsar radio emission is not well understood. It is generally thought that the radio emission is generated in an electron-positron plasma that is created from a pair cascade near the pulsar polar cap (e.g., Ref. [1]). The plasma, which we call the pulsar plasma, flows along open field lines with a bulk relativistic velocity. The specific mechanism for production of pulsar plasma involves acceleration of primary electrons (or positrons) to ultrarelativistic energy along the open field lines by a rotation-induced parallel electric field [2–5]. These ultrarelativistic primary particles radiate high-energy γ rays, which decay into electron-positron pairs in strong pulsar magnetic fields. These pairs together with primary particles form a relativistic plasma that flows out along the open field lines.

There are extensive discussions in the literature on the wave properties in the pulsar plasma [6–14]. However, the pulsar plasma remains poorly understood. Most of these earlier studies assumed a nongyrotropic plasma, that is, one that contains equal numbers of electrons and positrons with the same distribution functions. An important implication of this assumption is that all relevant waves are linearly polarized [7–9]. In practice, charge imbalance must occur, mainly due to the primary beam [2–4], or relative motion of electrons and positrons, implying that the distributions of bulk electrons and positrons are not identical [10]. When the distribution functions of electrons and positrons are not the same, the plasma is gyrotropic, implying that the natural wave modes are elliptically polarized in general.

Although pulsar radio emission is predominantly linearly polarized, a significant component of circular polarization is observed for most pulsars (e.g., Ref. [15]). One possible interpretation of circular polarization is that it reflects the ellipticity of the natural wave modes due to charge asymmetry [10,16–18].

Both the cyclotron effect and intrinsic relativistic effect were considered in a recent study of wave dispersion in pulsar plasmas in the nongyrotropic approximation [14]. Inclusion of the gyrotropic terms was recently considered in Ref. [18] in the low-frequency approximation, corresponding to wave frequencies much lower than the cyclotron frequency. The cyclotron effect needs to be considered for two reasons. (i) The radio emission generated near the polar cap must propagate outward through a region with a much weaker magnetic field where the cyclotron resonance condition is satisfied. (ii) For some pulsars the radio emission may be produced far from the polar cap, near or in the cyclotron resonance region [19,20]. Inclusion of the cyclotron resonance effects on the properties of the known (O and X) wave modes allows cyclotron absorption to occur [19,20], and in principle it can also lead to additional modes [14].

In this paper we consider wave dispersion in an intrinsically relativistic, gyrotropic pulsar plasma with the gyrotropic terms arising from the imbalance between the electron and positron number densities. In particular, we discuss elliptical polarization resulting from the gyrotropic terms, and we include the cyclotron resonance and gyrotropic terms. We discuss the possibility that the elliptical polarization due to the gyrotropic terms can lead to the observed circular polarization in pulsar radio emission.

In Sec. II, the general formulas for the dielectric tensor in terms of the relativistic plasma dispersion functions (RPDFs) are outlined with emphasis on the gyrotropic terms. In Sec. III, modified power-law distributions are introduced and the three RPDFs are evaluated both analytically and numerically in the plasma rest frame. Wave dispersion and polarization for a gyrotropic pulsar plasma are discussed in detail in Sec. IV.

II. THE DIELECTRIC TENSOR

Plasma dispersion can be obtained from the dielectric tensor, which can be derived in the one-dimensional approximation for a pulsar plasma. In the strong pulsar magnetic field electrons (positrons) relax to their ground Landau states. Cyclotron absorption involves transitions between the ground and first excited Landau states and we include this process in treating the escape of the radiation. However, the number of electrons or positrons in the first excited state is assumed to be small and can be neglected.

*Electronic address: q.luo@physics.usyd.edu.au

 ©2002 The American Physical Society

The dielectric tensor for relativistic pulsar plasmas can be written in terms of three relativistic plasma dispersion functions [11,12,14]. We summarize here the relevant formulas with emphasis on the gyrotropic terms. The relevant resonances are described by $\omega - k_\parallel v - s\Omega_e/\gamma = 0$ with $s = 0, -1$, and 1 corresponding, respectively, to the Čerenkov, anomalous cyclotron, and normal cyclotron resonances, where Ω_e is the cyclotron frequency. Let $z = \omega/k_\parallel$ be the parallel phase velocity (we set $c = 1$) and $y = \Omega_e/k_\parallel$. There are two solutions to the cyclotron condition (anomalous or normal cyclotron resonance): $z_\pm = [z \pm y(1 + y^2 - z^2)^{1/2}]/(1 + y^2)$. There are three parameter regions of interest: $z < 1$, $1 < z < (1+y^2)^{1/2}$, and $z > (1+y^2)^{1/2}$. The Čerenkov and anomalous cyclotron resonances can occur in the first region and the normal cyclotron resonance is allowed in the first and second regions. There is no resonance in the third region. In the following discussion we consider only the regions with $z < (1+y^2)^{1/2}$.

The dielectric tensor can be written into the form [14]

$$K_{11} = K_{22} = 1 - \frac{\omega_p^2}{\omega^2}\frac{1}{1+y^2}\left[\left\langle\frac{1}{\gamma}\right\rangle + \sum_{\alpha=\pm}\frac{\alpha(z-z_\alpha)^2 R(z_\alpha)}{z_+ - z_-}\right], \tag{1}$$

$$K_{12} = -K_{21} = -\frac{i\eta\omega_p^2}{\omega^2}\frac{y}{(1+y^2)}\sum_{\alpha=\pm}\frac{\alpha(z-z_\alpha)S(z_\alpha)}{z_+ - z_-}, \tag{2}$$

$$K_{13} = K_{31} = -\frac{\omega_p^2}{\omega^2}\frac{\tan\theta}{(1+y^2)} \times\left[-\left\langle\frac{1}{\gamma}\right\rangle + \sum_{\alpha=\pm}\frac{\alpha z_\alpha (z-z_\alpha)R(z_\alpha)}{z_+ - z_-}\right], \tag{3}$$

$$K_{23} = -K_{32} = \frac{i\eta\omega_p^2}{\omega^2}\frac{y\tan\theta}{(1+y^2)}\sum_{\alpha=\pm}\frac{\alpha z_\alpha S(z_\alpha)}{z_+ - z_-}, \tag{4}$$

$$K_{33} = 1 - \frac{\omega_p^2 z^2}{\omega^2}W(z) + \frac{\omega_p^2}{\omega^2}\frac{\tan^2\theta}{1+y^2}\left[\left\langle\frac{1}{\gamma}\right\rangle + \sum_{\alpha=\pm}\frac{\alpha z_\alpha^2 R(z_\alpha)}{z_+ - z_-}\right], \tag{5}$$

where $W(z)$, $R(z)$, and $S(z)$ are the RPDFs, $\omega_p = [4\pi e^2(n_+ + n_-)/m_e]^{1/2}$, $\eta = (n_+ - n_-)/(n_+ + n_-)$, the angular brackets denote the average over the particle distribution, and $n_\pm$ are the positron and electron number densities. We assume that the plasma contains only electrons and positrons, and that the wave vector is in the 1-3 plane at an angle θ relative to the ambient magnetic field, which is assumed to be along the 3 axis. The three RPDFs are defined by

$$W(z) = \int_{-\infty}^{\infty} F'(u)\frac{du}{v - z}, \tag{6}$$

$$R(z) = \int_{-\infty}^{\infty} F(u)\frac{du}{\gamma(v-z)}, \tag{7}$$

$$S(z) = \int_{-\infty}^{\infty} F(u)\frac{du}{\gamma^2(v-z)}. \tag{8}$$

The distribution function $F(u)$ is normalized to 1, where u is the dimensionless momentum ($u = \gamma v$). Calculation of the response reduces to evaluation of the three RPDFs. The plasma is said to be intrinsically relativistic if in the plasma rest frame the condition $\Delta v^2 \equiv 1 - \langle 1/\gamma\rangle/\langle\gamma\rangle \ll 1$ is *not* satisfied. The cold plasma limit corresponds to $\Delta v^2 = 0$.

III. RELATIVISTIC DISTRIBUTIONS AND RPDFS

A specific form of plasma distribution is required to evaluate the RPDFs. However, the actual distribution of secondary pair plasmas in pulsars is not well understood, mainly because the distribution strongly depends on the model of primary particle acceleration and the structure of the pair formation region [21–23]. Several types of distribution have been considered. These include a relativistic Maxwellian distribution (the Jüttner distribution) [12,24,25], a bell-type distribution [11], the water-bag distribution [9], and a power-law distribution. The water-bag distribution has a cutoff, at v_m say, and this causes the RPDFs to be singular at $z = v_m$. The bell-type distributions smooth out the singularity, whose effects are entirely absent only for the Jüttner distribution.

To calculate the RPDFs we consider the plasma rest frame and introduce a power-law-like distribution given by

$$F(u) = N_p\gamma^{-p}(\gamma_m^2 - \gamma^2)^2, \quad -u_m \leqslant u \leqslant u_m, \tag{9}$$

where u_m is the cutoff, with $\gamma_m = (1+u_m^2)^{1/2} = 1/(1-v_m^2)^{1/2}$. We call the distribution a modified power-law (MPL) distribution. It resembles a power-law distribution but gives rise to RPDFs that are continuous at the cutoff $v = v_m$ (Fig. 1). The special case $p = 0$ corresponds to the soft-bell distribution [11]. The normalization constant N_p is given by

$$N_p = \left[\int_{-v_m}^{v_m} dv\ \gamma^{-p+3}(\gamma_m^2 - \gamma^2)^2\right]^{-1}. \tag{10}$$

For $p = 0, \pm 1, 2, 3$ we have

$$N_0 = 15/(16u_m^5), \tag{11}$$

$$N_1 = 4[-3u_m\gamma_m(1+2u_m^2) + (3+8u_m^2\gamma_m^2)\operatorname{arcsinh} u_m]^{-1}, \tag{12}$$

$$N_{-1} = 24[u_m\gamma_m(8u_m^4 - 10u_m^2 - 3) + 3(8u_m^4 + 4u_m^2 + 1)\sinh^{-1} u_m]^{-1}, \tag{13}$$

$$N_2 = \left[-\frac{2}{3}u_m(3+5u_m) + 2\gamma_m^4\arctan u_m\right]^{-1}, \tag{14}$$

$$N_3 = [u_m\gamma_m(3+2u_m^2) - (3+4u_m^2)\operatorname{arcsinh} u_m]^{-1}. \tag{15}$$

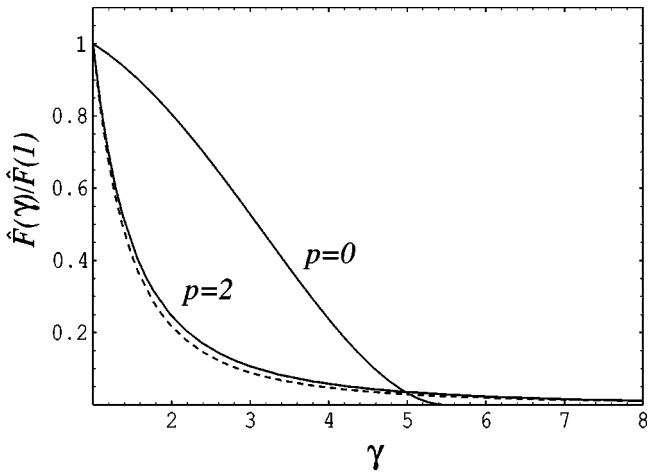

FIG. 1. The MPL distributions (relative scale). A symmetric distribution with $F(u)=F(-u)$ can be written as $\hat{F}(\gamma)=F([1-1/\gamma^2]^{1/2}\gamma)$. The dashed curve is a simple power-law distribution (γ^{-p}) with $p=2.2$. The soft-bell distribution can be regarded as a special case of the MPL distributions ($p=0$). We assume $\gamma_m=5.5$ for the soft-bell distribution and $\gamma_m=20$ for the MPL distribution. In both cases we have $\langle\gamma\rangle\approx 2$.

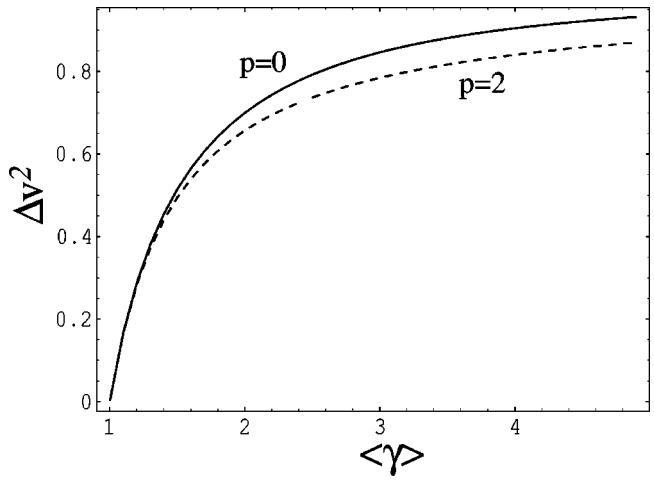

FIG. 2. The mean square velocity (Δv^2) vs $\langle\gamma\rangle$ for the soft-bell (solid curve) and MPL (dashed curve) distributions.

For a given p, the two relevant averages $\langle 1/\gamma\rangle$ and $\langle\gamma\rangle$ can be written in the forms

$$\left\langle\frac{1}{\gamma}\right\rangle = N_p/N_{p+1}, \tag{16}$$

$$\langle\gamma\rangle = N_p/N_{p-1}. \tag{17}$$

The mean square speed is then given by $\Delta v^2 = 1 - N_{p-1}/N_{p+1}$.

The distributions with $p>0$ appear intrinsically less relativistic than that with $p=0$. Figure 2 shows plots of Δv^2 against $\langle\gamma\rangle$. For a given $\langle\gamma\rangle$ the corresponding mean square speed is generally lower for the distribution with $p=2$ than that for the soft-bell distribution. This "softness" leads to RPDFs with relatively broader peaks (see the discussion in the following section).

A. RPDFs for a soft-bell distribution

The soft-bell distribution ($p=0$) was discussed in detail in Refs. [11,12,14]. The analytic expressions for two of the RPDFs, $W(z)$ and $R(z)$, are known [14]:

$$W(z)=\frac{15}{32v_m^5\gamma_m(1-z^2)}\left[2v_m+\frac{2v_m}{1-z^2}(4z^2-3v_m^2-z^2v_m^2)+(3z^4+6z^2-1+v_m^2z^4-3v_m^2-6v_m^2z^2)\frac{1-v_m^2}{(1-z^2)^2}\ln\left|\frac{1+v_m}{1-v_m}\right|\right.$$
$$\left.+\frac{8z}{\gamma_m^2}\frac{(v_m^2-z^2)}{(1-z^2)^2}\ln\left|\frac{v_m+z}{v_m-z}\right|\right]-i\pi\frac{15z(u_m^2-u_0^2)}{4u_m^5(1-z^2)^2}H(v_m-z), \tag{18}$$

$$R(z)=\frac{15\gamma_z^6}{128v_m^5\gamma_m}\left\{-2zv_m[(7v_m^2-1)-2z^2(1+5v_m^2)+3z^4(1+v_m^2)]+z[v_m^4(15-10z^2+3z^4)-v_m^2(6+12z^2-2z^4)-1+3z^4\right.$$
$$\left.+6z^2]\ln\left|\frac{1+v_m}{1-v_m}\right|-8(v_m^2-z^2)^2\ln\left|\frac{v_m+z}{v_m-z}\right|\right\}+i\pi\frac{15\gamma_z^6}{16v_m^5\gamma_m}(v_m^2-z^2)^2H(v_m-z), \tag{19}$$

where $\gamma_z=(1-z^2)^{1/2}$ for $|z|\leqslant 1$ and for $R(z)$ the relevant region is $|z|\leqslant 1$. The properties of $W(z)$ for both Jüttner and bell-type distributions were considered in detail in Ref. [12]. The third RPDF, $S(z)$, is derived in a similar way to the derivation of $W(z)$ and $R(z)$ [11,12,14]:

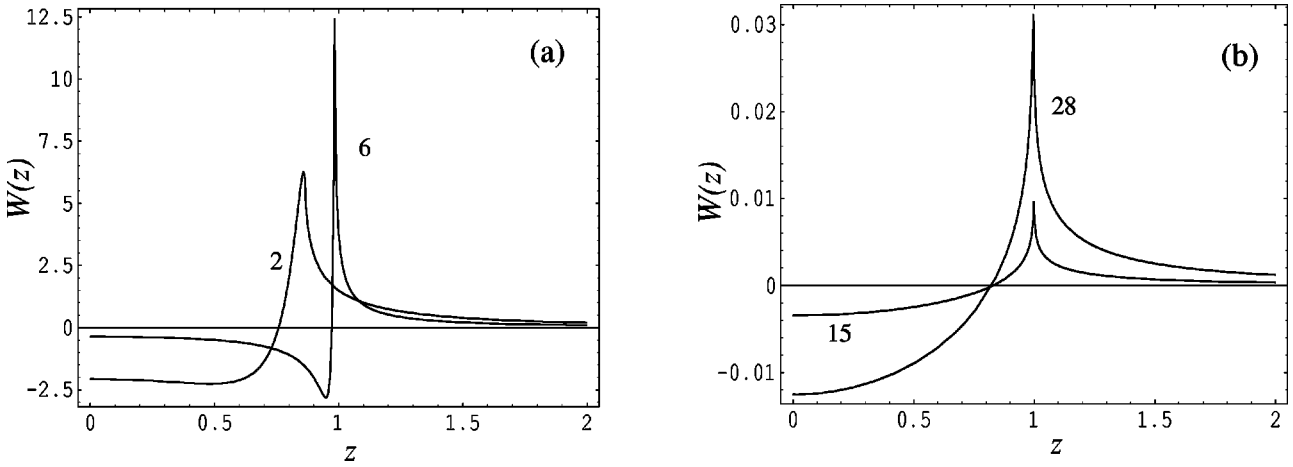

FIG. 3. The relativistic dispersion function $W(z)$. (a) A soft-bell distribution with $\gamma_m=2$ ($\langle\gamma\rangle=1.2$) and $6(\langle\gamma\rangle=2.2)$. The curve with the sharper peak corresponds to the distribution with $\gamma_m=6$. (b) A MPL distribution of $p=2$. We choose $\gamma_m=15$ and $\gamma_m=28$ such that $\langle\gamma\rangle \approx 1.9$ and 2.2. In contrast to (a), here there is no negative peak.

$$S(z)=\frac{5(\gamma_z\gamma_m)^4}{16u_m^5}\left[2(3z^2-5v_m^2+2v_m^2z^2)\frac{v_mz}{\gamma_m}+\frac{3(v_m^2-z^2)^2}{(1-z^2)^{1/2}}\times\ln\left|\frac{(1+v_mz)\gamma_m\gamma_z+1}{(1-v_mz)\gamma_m\gamma_z+1}\,\frac{v_m-z}{v_m+z}\right|\right]+i\frac{15\gamma_z}{16u_m^5}F(z\gamma_z). \tag{20}$$

Notice that $S(z)$ is continuous at $z=v_m$ and as for $R(z)$ only the region $|z|\leqslant 1$ is relevant for the calculation of the dielectric tensor.

For $p=0$ Eqs. (14) and (15) give

$$\left\langle\frac{1}{\gamma}\right\rangle=N_0/N_1=\frac{15}{128v_m^5\gamma_m}\left[(3+2v_m^2+3v_m^4)\ln\left|\frac{1+v_m}{1-v_m}\right|-6v_m(1+v_m^2)\right]. \tag{21}$$

The average Lorentz factor is given by

$$\langle\gamma\rangle=N_0/N_{-1}=\frac{5}{128u_m^5}[u_m\gamma_m(8u_m^4-10u_m^2-3)+3(8u_m^4+4u_m^2+1)\sinh^{-1}u_m]. \tag{22}$$

B. RPDFs for MPL distributions

Analytical forms for the RPDFs can be obtained for a MPL distribution with a given integer p. Here we consider only $p=2$ as an example. The RPDFs are

$$W(z)=2N_2\gamma_m^2\left[-4v_m+\frac{1-v_m^2}{1-z^2}\ln\left(\frac{1+v_m}{1-v_m}\right)+2\frac{v_m^2-z^2}{1-z^2}\ln\left|\frac{v_m-z}{v_m+z}\right|\right]+4i\pi N_2\gamma_m^2z\left(1-\frac{\gamma_m^2}{\gamma_z^2}\right)\times H(v_m-z), \tag{23}$$

$$R(z)=-N_2\gamma_m^2\left\{\frac{z\gamma_z^2}{2\gamma_m^2}\left[2v_m-\left(3+v_m^2-\frac{2\gamma_z^2}{\gamma_m^2}\right)\times\ln\left(\frac{1+v_m}{1-v_m}\right)\right]+\left(1-\frac{\gamma_z^2}{\gamma_m^2}\right)^2\ln\left|\frac{v_m-z}{v_m+z}\right|\right\}+i\pi N_2(\gamma_z^2-\gamma_m^2)^2H(v_m-z), \tag{24}$$

$$S(z)=\frac{N_2\gamma_m^4}{\gamma_z}\left[2z\gamma_z\left(\frac{v_m}{\gamma_m^3}-\arcsin v_m\right)-\left(1-\frac{\gamma_z^2}{\gamma_m^2}\right)^2\times\ln\left|\frac{(1+v_mz)\gamma_z\gamma_m+1}{(1-v_mz)\gamma_z\gamma_m+1}\,\frac{v_m-z}{v_m+z}\right|\right]+i\pi\frac{N_2}{\gamma_z}(\gamma_z^2-\gamma_m^2)^2H(v_m-z), \tag{25}$$

where $u_z=z\gamma_z$.

The RPDFs are shown in Figs. 3(a) and 4(a) for the soft-bell distribution and Figs. 3(b) and 4(b) for the MPL distribution with $p=2$. As in the case of soft-bell distributions, $W(z)$ has a peak at $z=1$. Although $\langle\gamma\rangle$ has similar values in these two cases, for $p=2$, $W(z)$ has a much broader peak than for $p=0$ and the negative peak that is seen in Fig. 3(a) broadens to become invisible [cf. Fig. 3(b)].

Figures 4 show that the properties of $S(z)$ are very similar to those of $R(z)$ in that both of them are predominantly negative and peaked toward $z=1$. One has $S(1)=-1$ and

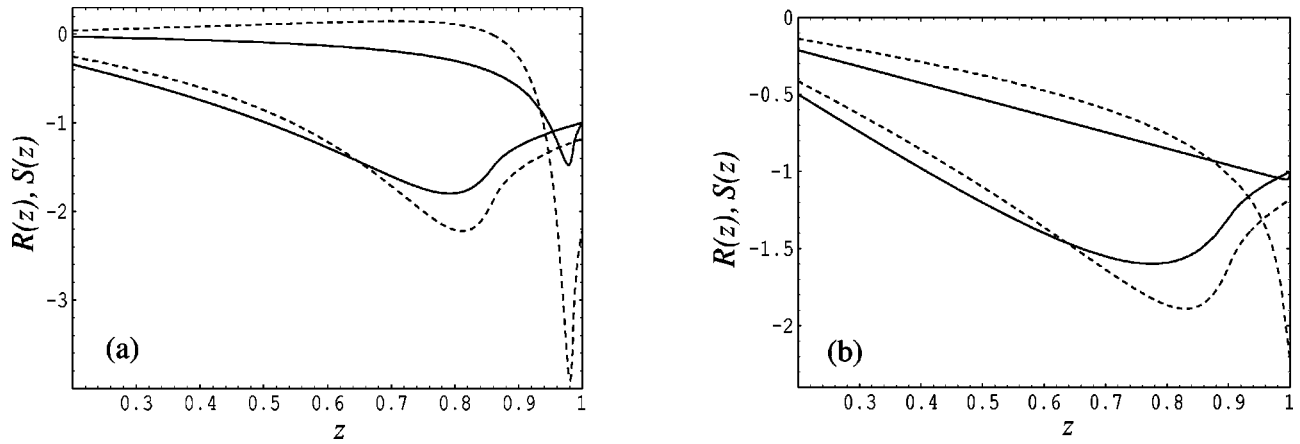

FIG. 4. Plots of $R(z)$ (dashed) and $S(z)$ (solid). (a) A soft-bell distribution with $\gamma_m=6$ (narrow peaks) and $\gamma_m=2$ (wide peaks). (b) A MPL distribution of $p=2$ for $\gamma_m=28$ (narrow peaks) and 2.4 (wide peaks). In both cases, the two functions are similar in that both of them are predominantly negative and peaked near $z=1$ for $\gamma_m \gg 1$. As $z\to 1$ we have $S(z)\to -1$. Note that in (b) $S(z)$ for $\gamma_m=28$ is peaked very near $z=1$ but as in (a) we have $S(z)\to -1$ for $z\to 1$.

$R(1)=-\langle\gamma\rangle$ as $z\to 1$ for any symmetric distribution [cf. Eqs. (7) and (8)]. For $p=2$, the peaks of $R(z)$ and $S(z)$ tend to be squashed toward $z=1$.

IV. WAVE PROPERTIES

A. Dispersion relations

Dispersion relations can be obtained as follows. Write $\Lambda_{ij}=(k^2/\omega^2)(\hat{k}_j\hat{k}_j-\delta_{ij})+K_{ij}^H$, where K_{ij}^H are the Hermitian parts of the dielectric tensor given by Eq. (5) and $\hat{k}_i=k_i/k$. The dispersion relation is then $\det(\Lambda_{ij})=(1/6)\varepsilon_{abc}\varepsilon_{ijl}\Lambda_{ia}\Lambda_{jb}\Lambda_{lc}=0$, where ε_{ijk} is the antisymmetric tensor. An analytic solution to the dispersion equation can be obtained only for some special cases such as the strong magnetic field approximation or nongyrotropic approximation, which were discussed, for example, by Volokitin *et al.* [7]. Here we solve the dispersion equation numerically using the RPDFs. Figure 5 shows dispersion relations for $\eta=0.1$. Since the pulsar magnetic field is generally assumed to be a dipole field, waves propagating initially parallel to the field line can acquire a finite angle. Thus, in the plasma rest frame the case of oblique propagation is the more plausible assumption. In Fig. 5 we assume $\theta=0.2$ for illustrative purposes.

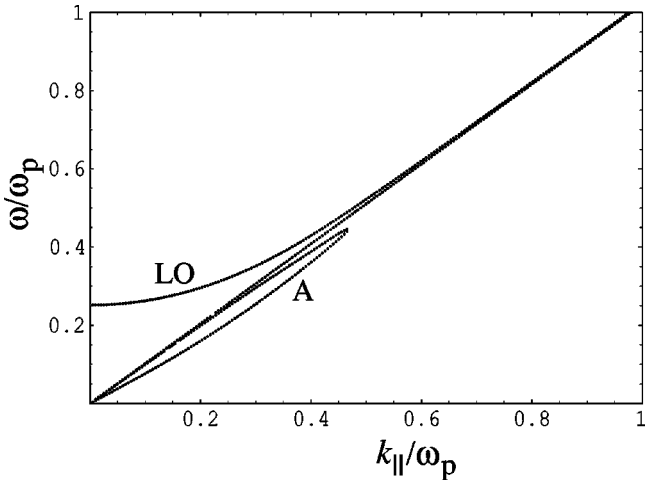

FIG. 5. Dispersion relations for a MPL distribution (with $p=2$) of a gyrotropic electron-positron plasma. We assume $\gamma_m=3$, $\omega_p/\Omega_e=0.01$, $\eta=0.1$, and $\theta=0.2$. The nearly straight line below the LO mode is the X mode.

The dispersion curves have similar features to that for a nongyrotropic plasma [14], showing three distinct modes: the LO mode, which has a cutoff at $\omega_c=\omega_p\langle\gamma^{-3}\rangle^{1/2}$, the X mode, which is close to the light line, and the low-frequency Alfvén mode, which is subject to strong damping at high frequency. Note that the distribution function in the pulsar frame is in general asymmetric about the origin ($u=0$) and that technically the forward and backward waves may be treated separately. Nonetheless, since only the forward waves (in the pulsar frame) are of interest here, such subtlety will not be discussed further. Since inclusion of a small charge asymmetry $\eta \ll 1$ introduces terms of the order $\eta^2 \ll 1$ into the dispersion relations, it does not affect the dispersion curves very much apart from change of the cutoff frequencies. However, the gyrotropic effect does change the polarization significantly (see the discussion in the next section).

The relevant cutoffs, which correspond to $k_\parallel=0$, can be estimated by formally taking the large z and y limits. The dielectric tensor can be approximated by

$$K_{11}=K_{22}=1+\frac{\omega_p^2}{\omega^2}\frac{1}{1+y^2}[\langle\gamma v^2\rangle+z^2\langle\gamma\rangle]$$

$$=1+\frac{\omega_p^2}{\Omega_e^2}\left[\frac{1}{z^2}\langle\gamma v^2\rangle+\langle\gamma\rangle\right], \tag{26}$$

$$K_{12}=-K_{21}=\frac{i\eta\omega_p^2}{\omega^2}\frac{yz}{(1+y^2)}=\frac{i\eta\omega_p^2}{\omega\Omega_e}, \tag{27}$$

$$K_{13}=K_{31}=-\frac{\omega_p^2\tan\theta}{z^2\Omega_e^2}\langle\gamma v^2\rangle, \tag{28}$$

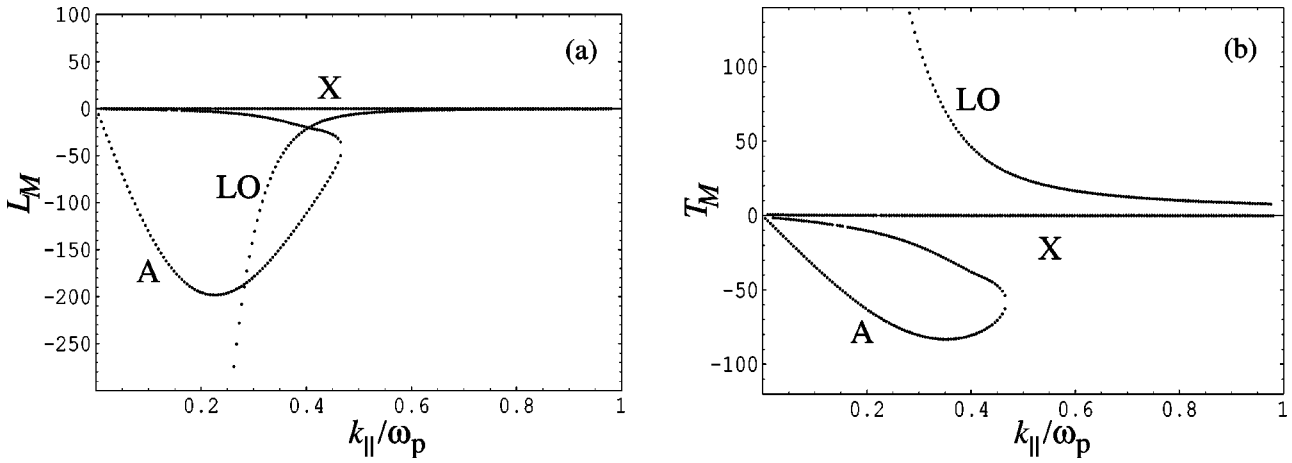

FIG. 6. Polarization coefficients vs $k_\parallel$. The LO mode is approximately longitudinal at small $k_\parallel$ (i.e., $|L_{LO}| \gg |T_{LO}| \gg 1$). Note that for the X mode both T_X and L_X are nonzero (cf. Figs. 7 and 10 below). The plasma parameters are the same as in Fig. 5.

$$K_{23} = -K_{32} = 0, \tag{29}$$

$$K_{33} = 1 - \frac{\omega_p^2 z^2}{\omega^2} W(z) + \frac{\omega_p^2 \tan^2\theta}{z^2 \Omega_e^2} \langle \gamma v^2 \rangle, \tag{30}$$

where $z_\pm \to \pm 1$, $R(\pm 1) = \mp\langle\gamma\rangle - \langle\gamma v\rangle = \mp\langle\gamma\rangle$, $S(\pm 1) = \mp 1 - \langle v\rangle = \mp 1$, and $\langle \gamma v^2 \rangle = -\langle \gamma^{-1} \rangle + \langle v \rangle$. Assuming $k_\parallel = 0$ we have two equations, $K_{33} = 0$, which determines the usual cutoff of the LO mode, and $K_{11} = \pm K_{12}$, which determines all other cutoffs that are affected by the gyrotropic term. For the LO mode, the cutoff is determined by $1 - (\omega_p/\omega)^2 z^2 W(z) = 0$ in the limit $z \to \infty$. Since $z^2 W(z) \to \langle \gamma^{-3} \rangle$ for $z \to \infty$ one finds $\omega_c = \omega_p \langle \gamma^{-3} \rangle^{1/2}$ [12].

There are also cutoff frequencies at $\omega_\pm/\Omega_e = \pm \eta (\omega_p/\Omega_e)^2 / (1 + \omega_p^2 \langle\gamma\rangle / \Omega_e^2) \approx \pm \eta (\omega_p/\Omega_e)^2$, where the approximation applies for $\omega_p \langle\gamma\rangle / \Omega_e \ll 1$. This result is very similar to that obtained in Refs. [26,27] for a cold, asymmetric electron-positron plasma. For $\eta = 0.1$, $\omega_p/\Omega_e = 0.1$, we have $\omega_\pm/\Omega_e \approx 10^{-3}$.

B. Polarization

The wave polarization vector can be obtained as follows using the formal procedure described in Ref. [28]. We write the polarization vector in the form

$$\mathbf{e}_M = \frac{L_M \hat{\mathbf{k}} + T_M \hat{\mathbf{t}} + i \hat{\mathbf{a}}}{(L_M^2 + T_M^2 + 1)^{1/2}}, \tag{31}$$

where $\hat{\mathbf{k}} = (\sin\theta, 0, \cos\theta)$, $\hat{\mathbf{t}} = (\cos\theta, 0, -\sin\theta)$, and $\hat{\mathbf{a}} = (0,1,0)$. The longitudinal part L_M and the axial ratio T_M are given by

$$T_M = i \frac{\mathbf{e}_M \cdot \hat{\mathbf{t}}}{\mathbf{e}_M \cdot \hat{\mathbf{a}}} = i \frac{\lambda_{1j} \cos\theta - \lambda_{3j} \sin\theta}{\lambda_{2j}}, \tag{32}$$

$$L_M = i \frac{\mathbf{e}_M \cdot \hat{\mathbf{k}}}{\mathbf{e}_M \cdot \hat{\mathbf{a}}} = i \frac{\lambda_{1j} \sin\theta + \lambda_{3j} \cos\theta}{\lambda_{2j}}, \tag{33}$$

where $\lambda_{ij} = (1/2) \varepsilon_{iab} \varepsilon_{jrs} \Lambda_{ra} \Lambda_{sb}$, and where the dispersion relation is implicit. For example, choosing $j = 2$, we obtain

$$\mathbf{e}_M = \frac{(\lambda_{1j}, \lambda_{2j}, \lambda_{3j})}{(\lambda_{1j}^2 + \lambda_{2j}^2 + \lambda_{3j}^2)^{1/2}},$$

$$\lambda_{ij} = (1/2) \varepsilon_{iab} \varepsilon_{jrs} \Lambda_{ra} \Lambda_{sb}, \tag{34}$$

provided that $\lambda_{1j}^2 + \lambda_{2j}^2 + \lambda_{3j}^2 \neq 0$. It is sometimes convenient to use

$$\lambda_{12} = \left(\frac{\tan\theta}{z^2} + K_{13} \right) K_{32} + \left(\frac{\tan^2\theta}{z^2} - K_{33} \right) K_{12}, \tag{35}$$

$$\lambda_{22} = \left(\frac{1}{z^2} - K_{11} \right) \left(\frac{\tan^2\theta}{z^2} - K_{33} \right) - \left(\frac{\tan\theta}{z^2} + K_{13} \right)^2, \tag{36}$$

$$\lambda_{32} = \left(\frac{\tan\theta}{z^2} + K_{13} \right) K_{12} + \left(\frac{1}{z^2} - K_{11} \right) K_{32}. \tag{37}$$

In the nongyrotropic approximation ($K_{12} = K_{32} = 0$), one has $\lambda_{12} = 0$, giving $L_X = T_X = 0$ for the X mode. The wave is purely transverse with polarization along $\hat{\mathbf{a}}$. Thus, in the one-dimensional approximation, particles that move strictly along the field lines cannot interact effectively with this mode through Čerenkov resonance since the electric field of the wave is perpendicular to the direction of particle motion. For the LO mode, owing to the dispersion relation $\lambda_{22} = 0$, both T_{LO} and L_{LO} are in general nonzero and hence the polarization is in the $\hat{\mathbf{k}}$-$\hat{\mathbf{t}}$ plane. [It is convenient to obtain T_{LO} and L_{LO} by choosing $j = 1$ or 3 in Eqs. (32) and (33).] Since $\mathbf{e}_{LO}$ has a component along the ambient magnetic field, these particles can interact with the subluminal LO mode in the Čerenkov resonance.

In the gyrotropic case, polarization is in general a mix of the three components along $\hat{\mathbf{k}}$, $\hat{\mathbf{t}}$, and $\hat{\mathbf{a}}$ and hence the relevant modes are elliptically polarized. Figure 6 shows the

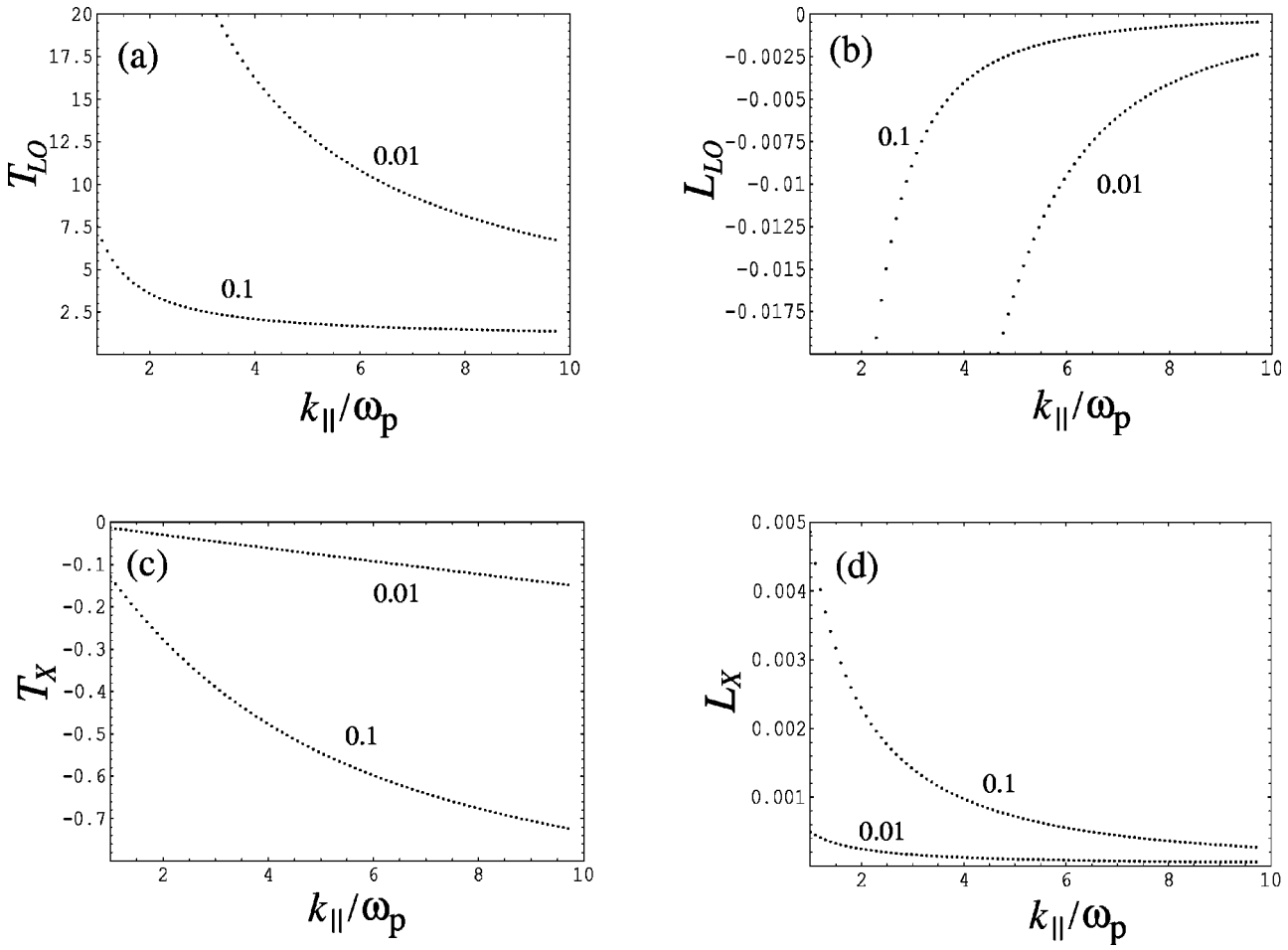

FIG. 7. Polarization coefficients for the LO and X modes for $\eta=0.1$ and 0.01. The upper and lower panels correspond, respectively, to the LO and X modes. The parameters are as in Fig. 5. The two modes are approximately orthogonal, $T_X T_{LO}\approx -1$ (cf. Fig. 9 below).

polarization coefficients for the three modes as a function of $k_\parallel$ for $\eta=0.1$, $\Omega_e=10^{-2}\omega_p$, and $\theta=0.2$. The corresponding dispersion relations are shown in Fig. 5.

The LO mode is predominantly polarized in the $\hat{\mathbf{k}}$-$\hat{\mathbf{t}}$ plane with a small polarization component along $\hat{\mathbf{a}}$. The mode is elliptically polarized with the ellipticity T_{LO}. The LO mode is longitudinal at small $k_\parallel$ and becomes transverse as frequency increases (cf. Fig. 7). Like the LO mode, the Alfvén mode is predominantly polarized in the $\hat{\mathbf{k}}$-$\hat{\mathbf{t}}$ plane but with a considerably larger component along the $\hat{\mathbf{a}}$ direction than the LO mode at low frequencies. The upper and lower branches have different polarization features (as shown in Fig. 8, which is obtained using the same parameters as those in Fig. 5); the upper branch has mostly $T_A > L_A$, while the lower branch is mainly longitudinal.

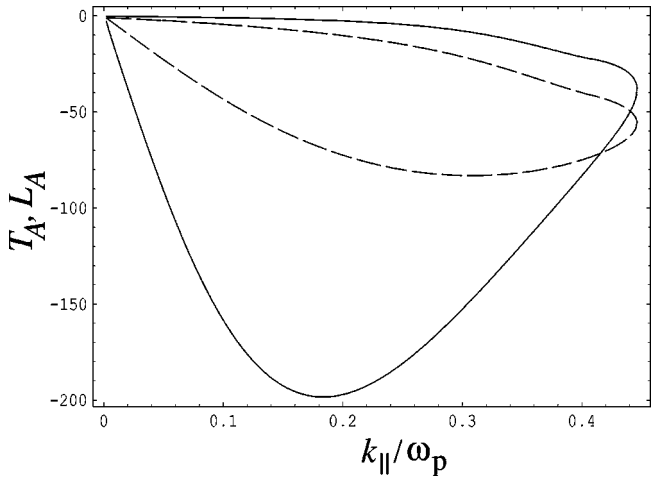

FIG. 8. Polarization coefficients T_A (dashed) and L_A (solid) for the Alfvén mode. The parameters are the same as in Fig. 5.

In contrast to the nongyrotropic case, the X mode has a significant longitudinal component ($L_X\neq 0$), which decreases for increasing ω/ω_p. A small electrostatic component remains even for frequencies much higher than ω_p (cf. Fig. 7). The X mode is known to have subluminal regions [14]. The elliptically polarized X mode has a nonzero component parallel to the ambient magnetic field. Therefore, when gyrotropy is included, the X mode can interact with particles in the Čerenkov resonance in the same way as for the LO mode. It is known that the dispersion equation for a cold plasma is quadratic in the square of the refraction index, n^2. There is a pair of solutions $n_\pm^2$ with the polarization coefficients $T_\pm$ satisfying the orthogonal condition $T_+T_-=-1$ [28]. Such a condition is generally not satisfied by a

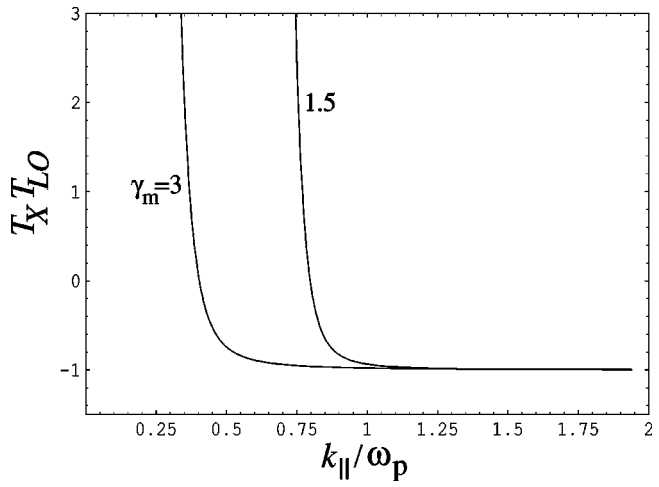

FIG. 9. Plots of $T_X T_{LO}$ as a function of $k_\parallel$ for $\gamma_m = 1.5$ and 3. As in Fig. 5 we assume $\omega_p/\Omega_e = 0.01$, $\theta = 0.2$, $\eta = 0.1$. The orthogonality ($T_X T_{LO} = -1$) holds for large $k_\parallel$.

thermal or a relativistic plasma because the dispersion equation has more than two solutions (e.g., the four dispersion curves in a certain range of $k_\parallel$; see Fig. 5). However, at high frequencies, there are only two dispersion curves, corresponding to the X and LO modes, respectively. Figure 9 shows that these two modes indeed satisfy the orthogonal condition for frequencies well above those for which the Alfvén mode is present. This result suggests that the dispersion equation at high frequencies can be approximately described by a quadratic equation for n^2 (square of refraction index).

The ellipticity for both the X and LO modes strongly depends on the propagation angle θ and the charge asymmetry η. For a small θ, only a small η is needed to produce nearly circular polarization. In general, θ is nonzero since waves progressively acquire angles relative to the curved field lines as they propagate outward. Thus, it is expected that in the plasma rest frame the propagation angle is oblique. As shown in Fig. 7, nearly circular polarization can be obtained for $\eta \geqslant 0.1$ (for $\theta = 0.2$).

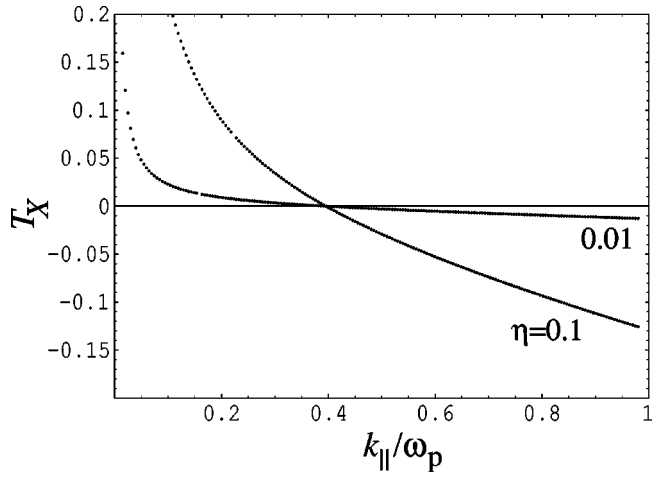

FIG. 10. An enlargement of T_X of Fig. 6. Note that the sign change occurs at $k_\parallel/\omega_p = 0.4$, which is approximately independent of η.

In the low-frequency region $\omega/\omega_p < 1$, a sign change occurs in T_X at $k_\parallel = 0.4$, implying a switch from one sense of elliptical polarization to the opposite. The frequency at which the polarization switches sign is not sensitive to η, as shown in Fig. 10. This can be understood from Eq. (24) from which the condition for sign change is $\lambda_{12}\cos\theta = \lambda_{32}\sin\theta$, that is, $K_{33}K_{12}\cos\theta = K_{11}K_{32}\sin\theta$. Since both K_{12} and K_{32} scale as η [cf. Eqs. (2) and (4)], this condition is independent of η for $z \approx 1$. In the cold plasma approximation, this frequency is just the plasma frequency ω_p.

C. Origin of the charge imbalance

One plausible mechanism for the origin of the charge imbalance is due to the presence of primary particles that have the Goldreich-Julian density particles, $n_{\rm GJ} = \mathbf{\Omega}\cdot\mathbf{B}/2\pi ce \approx 7\times 10^9 (0.1\ {\rm s}/P)(B/10^{12}\ {\rm G})\ {\rm cm}^{-3}$, where $\mathbf{\Omega}$ is the angular velocity of the neutron star and $\mathbf{B}$ is the magnetic field. Thus, one has $\eta \approx n_{\rm GJ}/2n_p = 1/2M$, where n_p is the pair number density and M is the multiplicity. Although the specific value of M is model dependent, a recent study [21] shows that polar cap acceleration alone may not produce a large M except for a few young pulsars that have extremely strong magnetic fields. Therefore most pulsars may have a low multiplicity and such charge asymmetry can lead to observable elliptical polarization.

Alternatively, charge asymmetry can be due to a difference between the electron and positron distributions. The effect associated with the difference in the distributions can be understood by considering the strong magnetic field limit $z_\pm \approx \pm 1$. Then, the gyrotropic components are $K_{12} = -K_{21} \propto z\eta - j$ and $K_{23} = -K_{32} \propto j$, where $j \equiv (n_+\langle v\rangle_+ - n_-\langle v\rangle_-)/(n_+ + n_-)$, and $\langle v\rangle_\pm$ are the average velocities for positrons and electrons, respectively. When the two distributions are different, say they have a shift relative to each other [18], the gyrotropic terms are nonzero even for $\eta = 0$ (i.e., the special case of equal number densities $n_+ = n_-$). The significance of these terms depends on the specific forms of the distributions, which are not well understood. In general, when a current is present, the gyrotropic terms with j need to be considered.

V. CONCLUSIONS AND DISCUSSION

We have considered wave dispersion of a gyrotropic pulsar plasma with the emphasis on elliptical polarization. A charge imbalance in relativistic electron-positron plasmas gives rise to an elliptically polarized mode. In deriving the plasma dispersion we use the three RPDFs to calculate the dielectric tensor. It is assumed that both electrons and positrons have the same distributions but different number densities. For a small charge asymmetry $\eta \ll 1$, apart from a change in the cutoff frequencies the dispersion curves remain very similar to those in the nongyrotropic case. However, the polarization can be quite different. The polarization coefficients for the LO mode and X mode are calculated for MPL distributions in the plasma frame. The result is summarized as follows.

(i) The RPDFs for a power-law distribution can be calculated approximately by using MPL distributions. For a MPL distribution the RPDFs are continuous at the cutoff v

$=\pm v_m$ and this avoids difficulties in numerical calculation of the dispersion relations.

(ii) As in the nongyrotropic approximation, there are three distinct modes: the LO mode, *X* mode, and low-frequency LO mode (or Alfvén mode). All three modes are elliptically polarized with both longitudinal and transverse components. In particular, for the *X* mode, which is purely transverse in the nongyrotropic approximation, the wave electric field has a component parallel to the pulsar magnetic field and therefore can interact with particles through Čerenkov resonance in the subluminal region.

(iii) The *X* and LO modes satisfy the orthogonal condition, i.e., $T_X T_{LO}=-1$, at frequencies higher than the maximum frequency of the Alfvén mode. The orthogonality implies that well above this frequency the dispersion equation is approximately quadratic in n^2, similar to that of cold plasmas, with the two solutions corresponding to the *X* and LO modes with $T_X T_{LO}\approx -1$. In the cold plasma approximation the orthogonal condition is satisfied for all frequencies.

(iv) In the low-frequency region ($\omega/\omega_p \leqslant 1$) the handedness of the elliptical polarization for the *X* mode reverses for $k_\parallel/\omega_p \approx 0.4$, irrespective of the charge imbalance η. In the cold plasma, the frequency at which the polarization sign reverses reduces to the plasma frequency. More generally, the ellipticity strongly depends on the charge imbalance η as well as the propagation angle. The polarization becomes more circular for increasing η or decreasing θ.

Although pulsar radio emission is mainly linearly polarized a significant component of circular polarization has been observed for many pulsars. The presence of nonzero ellipticity due to charge asymmetry provides a possible mechanism for the observed circular polarization. To obtain circular polarization, one requires either a low multiplicity or a small propagation angle. The latter condition may not be satisfied since the propagation angle is generally oblique owing to the field line curvature. Thus, the presence of circular polarization may require a relatively low multiplicity. Observations suggest that the radio emission may involve two orthogonal modes (*X* and LO), with the LO mode having a cutoff $\omega_c=\omega_p\langle\gamma^{-3}\rangle$. For the radio emission to be in the LO mode, the frequency must satisfy $\omega>\omega_c$, implying that low multiplicities are favored (at least in the propagation region). The low multiplicity is also required to avoid cyclotron absorption [29,20]. Figure 7 shows that nearly circular polarization can be obtained with $M\leqslant 10$ for $\theta=0.2$ (in the plasma rest frame). These parameters are well within the predicted range for polar cap models, e.g., Refs. [21,22].

So far, we have considered only wave properties modified by charge asymmetry due to imbalance in the number densities of electrons and positrons, within the frequency regime of $\omega/k_\parallel<(1+y^2)^{1/2}$. To apply our result to pulsars a further study of dispersion in gyrotropic plasmas is required, including the charge asymmetry arising from differences between the electron and positron distributions in momenta, as well as extending the frequency range to $\omega/k_\parallel\geqslant(1+y^2)^{1/2}$.

ACKNOWLEDGMENT

The authors thank the Australian Research Council (ARC) for financial support.

[1] D.B. Melrose, in *Pulsar Astronomy—2000 and Beyond*, edited by M. Kramer, N. Wex, and N. Wielebinski, ASP Conf. Ser. No. 202 (Astronomical Society of the Pacific, San Francisco, 2000), p. 721.
[2] P.A. Sturrock, Astrophys. J. **164**, 529 (1971).
[3] M.A. Ruderman and P.G. Sutherland, Astrophys. J. **196**, 51 (1975).
[4] J. Arons and E.T. Scharlemann, Astrophys. J. **231**, 854 (1979).
[5] J.K. Daugherty and A.K. Harding, Astrophys. J. **252**, 337 (1982).
[6] D.G. Lominadze, G.Z. Machabeli, and A.B. Mikhailovskii, Sov. J. Plasma Phys. **5**, 748 (1979).
[7] A.S. Volokitin, V.V. Krasnosel'shikh, and G.Z. Machabeli, Sov. J. Plasma Phys. **11**, 310 (1985).
[8] D.G. Lominadze, G.Z. Machabeli, G.I. Melikidze, and A.D. Pataraya, Sov. J. Plasma Phys. **12**, 712 (1986).
[9] J. Arons and J.J. Barnard, Astrophys. J. **302**, 120 (1986).
[10] A.Z. Kazbegi, G.Z. Machabeli, and G.I. Melikidze, Mon. Not. R. Astron. Soc. **253**, 377 (1991).
[11] M.E. Gedalin, D.B. Melrose, and E. Gruman, Phys. Rev. E **57**, 3399 (1998).
[12] D.B. Melrose *et al.*, J. Plasma Phys. **62**, 233 (1999).
[13] M. Lyutikov, G.Z. Machabeli, and R. Blandford, Astrophys. J. **512**, 804 (1999).
[14] M.P. Kennett, D.B. Melrose, and Q. Luo, J. Plasma Phys. **64**, 333 (2000).
[15] A. Lyne and R. Manchester, Mon. Not. R. Astron. Soc. **234**, 477 (1988).
[16] D.B. Melrose, Aust. J. Phys. **39**, A93 (1979).
[17] M.C. Allen and D.B. Melrose, Publ. Astron. Soc. Aust. **4**, 365 (1982).
[18] M. Gedalin, E. Gruman, and D.B. Melrose, Mon. Not. R. Astron. Soc. **325**, 715 (2001).
[19] R.D. Blandford and E.T. Scharlemann, Mon. Not. R. Astron. Soc. **174**, 59 (1976).
[20] Q. Luo and D.B. Melrose, Mon. Not. R. Astron. Soc. **325**, 187 (2001).
[21] J.A. Hibschman and J. Arons, Astrophys. J. **554**, 624 (2001).
[22] J.A. Hibschman and J. Arons, Astrophys. J. **560**, 871 (2001).
[23] S. Shibata, J. Miyazaki, and F. Takahara, Mon. Not. R. Astron. Soc. **295**, L53 (1998).
[24] J.C. Weatherall, Astrophys. J. **428**, 261 (1994).
[25] E. Asseo and A. Riazuelo, Mon. Not. R. Astron. Soc. **318**, 983 (2000).
[26] D.B. Melrose and M.E. Gedalin, Astrophys. J. **521**, 351 (1999).
[27] D.B. Melrose, Plasma Phys. Controlled Fusion **39**, A93 (1997).
[28] D.B. Melrose, *Plasma Astrophysics* (Gordon and Breach, New York, 1986), Vols. 1 and 2.
[29] Q. Luo, Publ. Astron. Soc. Aust. **18**, 400 (2001).